Phantom zircons provide new insights on the history of one of the oldest banded iron formation (BIF) on Earth (Isua greenstone belt, Greenland)

Quentin Aquila, Marion Garçon, Nicolas Olivier, Andrey Bekker

Phantom zircons provide new insights on the history of one of the oldest banded iron formation (BIF) on Earth (Isua greenstone belt, Greenland)

Quentin Aquila[1], Marion Garçon[1], Nicolas Olivier[1], Andrey Bekker[2]

[1]*Université Clermont Auvergne, CNRS, IRD,OPGC, Laboratoire Magmas et Volcans, F-63000 Clermont-Ferrand, France*

[2]*University of California Riverside, 900 University Ave, Riverside, CA 92521, USA*

To be submitted to Geochemica and Cosmochimica Acta

Abstract:

Banded Iron Formations (BIFs) offer a wide temporal and spatial window into the Precambrian seawater composition starting with the Eoarchean records. One of the oldest BIFs on Earth is preserved in the northeastern part of the ca. 3.7 Ga Isua Greenstone Belt (Greenland) in the Snowpatch Formation and this BIF unit has been used to generate the IF-G reference material (SARM, Nancy). The IF-G reference material is thought to record a primary seawater signature with no terrigenous contamination. Previous studies on Isua BIF have raised the paradox of the well-preserved, primary Pb isotopic composition along with the reset Nd isotopic composition. This study aims to distinguish primary vs. secondary signals imprinted in diverse mineralogy of the IF-G BIF by combining a petrological approach with trace element and Pb, Nd, and Hf isotopic analyses. Repeated analyses of trace element concentrations revealed a high variability induced by the heterogeneous grain-scale composition of the IF-G reference material. This heterogeneity is most pronounced in LREE, Zr, and Hf contents due to the nugget effect of apatite and zircon micro-grains. Pb isotopic composition of the IF-G reference material yields a well-defined ^{207}Pb-^{206}Pb isochron of 3810 ± 7 Ma (MSWD = 1.06), whereas the ^{176}Lu-^{177}Hf and ^{147}Sm-^{144}Nd isotopic systems are reset by post-depositional processes and/or result from a mixing of non-cogenetic minerals. We suggest that the 3810 Ma ^{207}Pb-^{206}Pb isochron reflects an average age of detrital zircons derived from a continental crust 110 Ma-older than the age of the BIF. The IF-G reference material yields an $\varepsilon Hf_{(3.7\ Ga)}$ > +100, which is unrealistically high for an Eoarchean BIF. Development of secondary apatite might have resulted in reset Hf and Nd isotopic signatures. Our findings signal that caution is required in interpreting records of highly metamorphosed Archean BIFs as seawater REE+Y patterns since chemical sedimentary rocks with Zr content as low as 1 ppm could contain zircon and thus are not entirely exempt of terrigenous contribution.

Keywords: Archean; Hf-Nd isotopic composition; Magnetite; Dating BIF; Seawater signature; Terrigenous contamination

1. Introduction

Banded iron formations (BIF) are Precambrian chemical sedimentary rocks that are widely used to explore the geochemistry of early oceans. They are interpreted as seawater precipitates and represent unique records of the environmental conditions that prevailed in the Archean oceans (e.g. Konhauser et al., 2017; Bekker et al., 2010, 2014). The largest preserved BIF deposits were deposited immediately before the GOE at ca. 2.5-2.45 Ga, but various economically significant occurrences are found from the Eoarchean to the end of the Proterozoic (Bau and Moller, 1993; Bau et al., 1996;Douville et al., 1999; Bolhar et al., 2004; Klein, 2005; Kato et al., 2006; Planavsky et al., 2010). These chemical sedimentary rocks consist of an alternation of mm- to cm-thick layers enriched in iron (Fe) and silicon (Si). Fe-oxides and quartz are the major constituents of BIF and the question of the hydrothermal vs. continental sources of Fe and Si to the early oceans has been hotly debated for decades (Holland, 1973; Michard, 1989; Isley, 1995; Isley and Abbott, 1999; André et al., 2006; Hamade et al., 2003; Wang et al., 2009; Bekker et al., 2010, 2014). Petrographic and geochemical constraints generally indicate low contribution of terrigenous input, suggesting deposition of BIFs in deep basins (Bekker et al., 2014; Klein, 2005; Konhauser et al., 2017). These sediments have the potential to record primary seawater signature similarly to modern Fe-Mn crusts (Albarède et al., 1998; van de Flierdt et al., 2004, 2007). Furthermore, despite generally low terrigenous contribution, their Hf and Nd isotopic composition might provide new insights into the chemical composition of emerged continents, the degree of continental weathering, and the sources of elements precipitated, as discussed by Viehmann et al. (2014, 2018).

This study is focused on the ca. 3.7 Ga-old IF-G reference material (SARM, Nancy), a BIF sampled from the Snowpatch Formation in the northeastern part of the Isua Greenstone Belt in Greenland (Appel, 1983; Govindaraju, 1984, 1995). The IF-G reference material is one of the oldest chemical sedimentary rocks known on Earth so far and therefore represents a unique record to study surface conditions in the Eoarchean. Based on a multi-elemental and multi-isotopic study (Sm-Nd, Lu-Hf, Pb), we discuss primary vs. secondary geochemical signatures, i.e., seawater composition vs. post-depositional metamorphism and/or alteration imprints that are relevant to provide insight into the age and the depositional environment of this unique archive. From the literature, we note

that the Snowpatch Formation BIF shows a rather intriguing isotopic feature where whole-rock ^{207}Pb-^{206}Pb isochrons point to Eoarchean dates (Moorbath et al., 1973; Frei et al., 1999; Frei and Polat, 2007), while other radiogenic systems, such as the ^{147}Sm-^{143}Nd and ^{138}La-^{138}Ce isotopic systems with closure temperatures higher than that of the ^{207}Pb-^{206}Pb isotopic system, yield surprisingly much younger dates (Shimizu et al., 1990; Frei et al., 1999; Frei and Polat, 2007). The latter authors inferred that younger metamorphic events are responsible for the growth of late REE-rich apatites that overprinted the BIF depositional age. First, our study aims to characterize the petrogeochemical features of this BIF reference material to evaluate its current use as a quality control standard. Secondly, we further explore the ^{207}Pb-^{206}Pb dates for the Isua BIF from the Snowpatch Formation by coupling Pb isotopic compositions with two more robust isotopic systems – ^{147}Sm-^{143}Nd and ^{176}Lu-^{176}Hf – to determine (1) which minerals control the Pb, Hf, and Nd isotopic composition of the Snowpatch Formation BIF; (2) whether the ^{207}Pb-^{206}Pb date is a metamorphic or depositional age, and (3) whether primary geochemical features have been preserved and provide insights into the depositional setting of one of the oldest BIF known on Earth.

2. Geological Context

The Isua Greenstone Belt is a part of the North Atlantic craton and contains a series of amphibolites derived from diverse mafic protoliths (Fig. 1). The Isua Greenstone Belt experienced several metamorphic events from the early Archean to early Proterozoic that were associated with emplacements of granitoids (Boak and Dymek, 1982; Bridgwater et al., 1973; Dymek and Klein, 1988; Nutman et al., 1997a; Nutman et al., 2022). The greenstone belt sedimentary rocks include felsic to mafic schists, BIFs, minor cherts, conglomerates, and carbonate rocks.

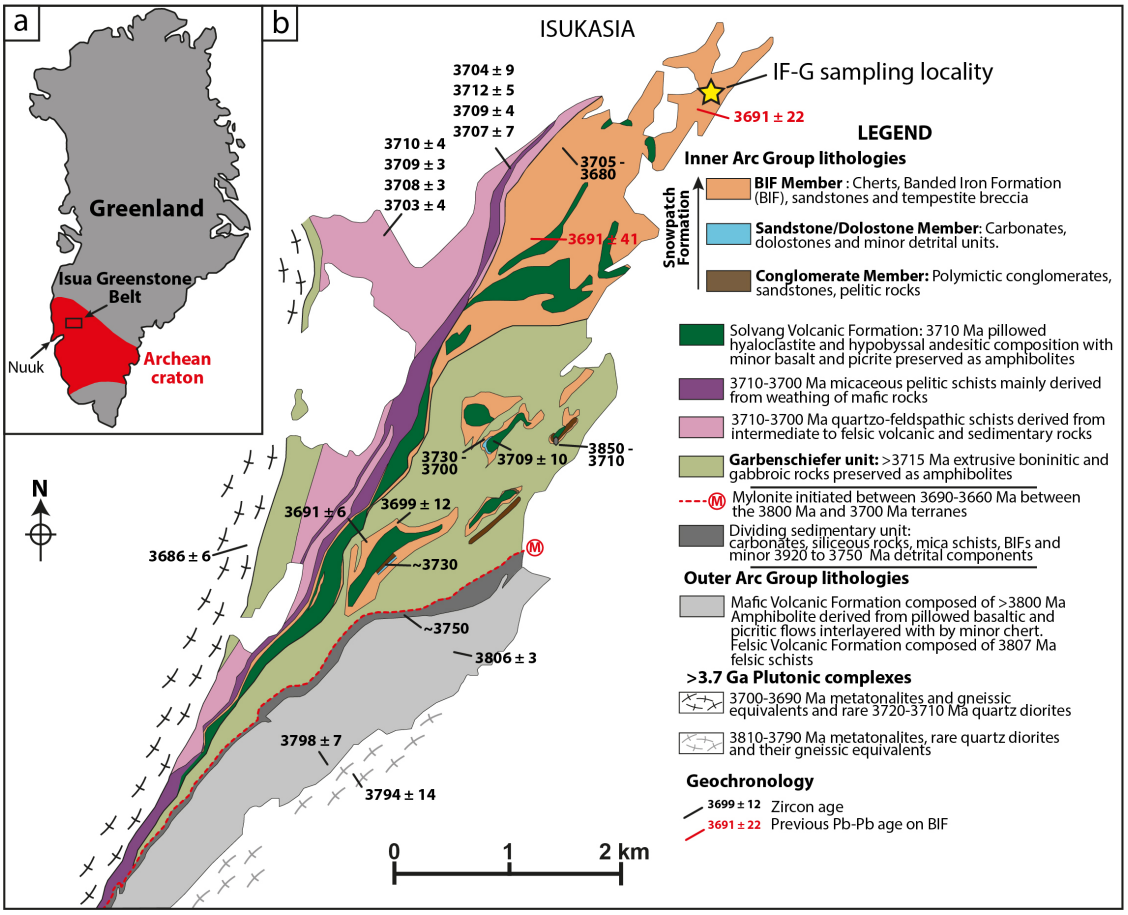

Fig.1. Maps showing geographical position and geological setting of the Northeastern Isua Greenstone Belt. (a) The Isua Greenstone Belt of the North Atlantic craton in Greenland. (b) Simplified geological map of the Northeastern Isua Greenstone Belt, adapted from Nutman et al. (2022). *U-Pb zircon ages are from* Nutman et al. (2022) *and references therein. Red arrows show* ^{207}Pb-^{206}Pb *dates determined for the northeastern BIF by* Frei et al. (1999) *and* Frei and Polat (2007). *Younger than 3.6 Ga magmatic intrusions are not shown on the map.*

The studied BIF sample, the IF-G reference material, belongs to the BIF Member within the Snowpatch Formation, which is a part of the ca. 3.7 Ga Inner arc Group (Fig. 1). The sample has been collected at the Iron Mountain locality in the most northeastern part of the belt (Appel, 1983). The sedimentary Snowpatch Formation was deposited unconformably on the Solvang Volcanic Formation, which is composed of chloritic schists and altered pillowed amphibolites with picritic, basaltic, and andesitic compositions (Polat & Hofmann, 2003). The age of the Solvang Volcanic Formation is constrained at ca. 3710 Ma (Nutman et al., 2010). The top of the Snowpatch Formation is defined by a tectonic contact with the older, over-thrusted, > 3715 Ma Garbenschiefer unit of boninitic and gabbroic rocks that are preserved as amphibolites (Komiya et al., 1999; Polat et al., 2002; Friend and Nutman, 2010).

The sedimentary Snowpatch Formation comprises in the ascending order: the Conglomerate, Sandstone/Dolostone, and BIF members (Fig. 1; Nutman et al., 2019). The Conglomerate Member is composed of conglomerates, sandstones and pelitic rocks and less than 25 m in thickness. The youngest dated zircon recovered from this member is 3710 Ma old. The Sandstone/Dolostone Member is a 50 m-thick succession composed of dolostones, sandstones, and a tempestite deposits. The BIF Member is a 100 m-thick succession of cherts with minor tempestite deposits and siliciclastic sandstones grading to a thick BIF unit (Nutman et al., 2019). The depositional age of the BIF Member is estimated to be ca. 3695 Ma (Nutman et al., 2009). Since the BIF unit in the BIF Member of the Snowpatch Formation is a unique BIF deposit for the entire formation, we will refer to them as the Snowpatch BIF.

The maximum metamorphic grade attained by the Northeastern Isua metasedimentary rocks, on which our study is focused, is estimated to be low amphibolite grade (Dymek and Klein, 1988; Nutman et al., 2022). However, the geochemical impact of such metamorphism on the Isua BIF is considered to be minimal because it records the typical trace-element signature of seawater precipitates (Bolhar et al., 2004a; Frei & Polat, 2007; Friend et al., 2008).

In the Isua greenstone belt, the inner arc has been dated and considered to consist of ca. 3.7 Ga metasediments separated from the ca. 3.8 Ga southern outer arc with a tectonic contact (mylonite) developed at ca. 3660 Ma (Nutman et al., 2022). The Snowpatch BIF were first dated at 3760 ± 70 Ma by Moorbath et al. (1973), using a ^{207}Pb-^{206}Pb isochron on bulk samples. This age was interpreted as a metamorphic age. Later, Frei et al. (1999)

dated hand-picked magnetite from the same unit with a ^{207}Pb-^{206}Pb isochron at 3691 ± 22 Ma. Recent studies dated scarce zircons in the Snowpatch Formation separated from the metaconglomerate, chert and BIF units with U-Pb ages of 3740 ± 8 Ma, 3694 ± 4 and 3707 ± 6 Ma, respectively (Nutman et al., 1997, 2002; Kamber et al., 2005). These dates constrain the depositional age of BIF from the Snowpatch Formation at ca. 3.7 Ga. Subsequently, new ^{207}Pb-^{206}Pb date for mesobands from the Snowpatch BIF of 3691 ± 49 Ma was interpreted as a depositional age (Frei and Polat, 2007), consistent with the previous ^{207}Pb-^{206}Pb dates for the Snowpatch BIF (Moorb@@ath et al., 1973; Frei et al., 1999). Most recent studies produced new detrital or volcanic zircon dates for the Snowpatch BIF that cluster at ca. 3.71-3.70 Ga (Fig. 1; Nutman et al., 2009, 2019).

3. Material and Methods

3.1. Material

All the analyses reported in this study were performed on a certified reference material from the SARM Nancy (France): the IF-G reference material, which is a ca. 3.7 Ga BIF deposit from the Iron Mountain area in the most northeastern part of the Isua Greenstone Belt, Greenland (Fig. 1). Petrographic observations were made on two thin sections from a rock sample and powder of IF-G provided by the SARM Nancy. Geochemical analyses were performed on the powder distributed by the SARM to the scientific community to be used as a reference BIF standard.

The IF-G standard is derived from one ton of the Iron Mountain ore body, which is estimated to host $2*10^9$ t of iron (Appel, 1980; Govindaraju, 1984). The large amount of rock material homogenized to prepare this standard makes it representative of the BIF Member of the Snowpatch Formation, and it is therefore a sample of choice to study the conditions under which such sediment was deposited in the Eoarchean. The IF-G reference material was crushed, powdered, quartered several times, and packaged into 30 g bags per 10 kg batch. Detailed information on the standard preparation can be found in Govindaraju (1984). Trace element contents and Nd isotopic composition have been previously analyzed and reported in the literature (Albut et al., 2018; Baker et al., 2002; Barrat et al., 2000; Bolhar et al., 2004a, 2005, 2015b; Dulski, 2001; Fabre et al., 2011; Frei et al., 2016; Friend et al., 2008; Govindaraju, 1995; Guilmette et al., 2009; Kamber et al., 2004; Parks et al., 2014; Sampaio & Enzweiler, 2015; Viehmann, Bau, Hoffmann, et al., 2015;

Viehmann, Bau, Smith, et al., 2015). Geochemical analyses (major and trace elements, and isotopic compositions) performed in this study were done on two different lots (IWG-GIT n°0600797 and n°0600998) that both escaped W, Co and Cr contamination generated by crushing facilities before 2006 as indicated in the certificates of analyses provided with the reference material (see Govindaraju 1984 for trace element data for lots produced before 2006).

3.2. Methods

The IF-G bulk powder was analyzed several times for major and trace elements, and isotopic compositions in this study. To better constrain mineralogical control on bulk chemical and isotopic compositions, individual mineral fractions separated from the bulk powder were also analyzed, and a detailed petrographic analysis of the bulk powder and two thin sections was performed using SEM imaging.

3.2.1. Magnetic separation to isolate individual mineral fractions

The fine-grained size and small amount of sample available (maximum 30 g per lot) make separation of individual mineral fractions through a Frantz magnetic separator and by hand-picking not possible. Instead, a first-order magnetic separation using a hand magnet and about 10 g of IF-G powder was performed. The powder was placed on a weighing paper and a hand magnet was covered by plastic film to avoid contamination during the separation procedure. The hand-magnet was positioned close to the powder to attract magnetic grains and isolate them from non-magnetic minerals. The procedure was repeated five times until the magnet had attracted all magnetic grains. Separation resulted in two fractions: (1) magnetite-rich fraction, still containing some silicate, phosphate, and carbonate grains; and (2) silicate-, phosphate-, and carbonate-rich fraction with some minor magnetite.

3.2.2. Scanning Electron Microscope (SEM) imaging

The IF-G bulk powder and the two thin sections were imaged and analyzed using a JEOL-JSM 5910-LV scanning electron microscope (SEM) equipped with a Quantax Xflash nanobruker energy-dispersive X-ray spectrometer (EDS). Samples were carbon-coated and the machine was operated at 15 kV for both backscattered electron imaging and EDS

chemical analysis. First, mineralogical composition and grain-size distribution of the powder were characterized. Maps of variable sizes (maximum 2.5 x 1.9 mm) were generated to get a qualitative estimate of Fe, Si, P, Mg, Ca, and S contents in the powder and grains.

3.2.3. Major element compositions

Major element contents were determined on 100 mg of sample powder digested by flux fusion using metaborate alkali fusion (about 400 mg of $LiBO_2$ for 100 mg of sample) and dissolved in diluted nitric acid (with dilution factor of about 2000). Solution were analyzed on an Inductively Coupled Plasma – Atomic Emission Spectrometer ICP-AES Agilent 5800 at the LMV of Clermont-Ferrand (France). Two geological reference standards BR (basalt) and GH (granite) were used to calibrate major element concentrations. Geological reference standards BHVO-1 (basalt) and DRN were used as quality control standards. Analytical errors for certified reference material BHVO-1 and DR-N were always below 3 % except for P_2O_5 where the error reached 10 % due to their low P_2O_5 contents (*c.f Chapitre 2 section 2.1*). Major element content of IF-G bulk powders was analyzed in three different sequences, and was duplicated in each sequence. The magnetite-rich and silicate-phosphate-carbonate-rich fractions were analyzed one time each in one sequence.

3.2.4. Trace element concentrations

Fourteen different dissolutions of IF-G bulk powder, three magnetite-rich fractions and three silicate-phosphate-carbonate-rich fractions were analyzed in this study. For the IF-G bulk powder, amount of powder dissolved ranged from 50 mg to 180 mg to test the representativeness of the powders. Except for three IF-G bulk powders, all samples were dissolved using NH_4HF_2 (ratio 1:4 for sample:flux) in Savillex® beakers heated in an oven at 215°C for at least 24 hours. This procedure ensures breaking of Si-O bounds and digestion of the most resistant minerals such as zircons, if present (Zhang et al., 2012). To assess efficiency of the digestion procedure, three IF-G bulk powders were digested in a mixture of 3 mL 29N HF + 1 mL 14N HNO_3 on a hot plate at 100 °C over 24 hours (samples named IFG-HF-B, IFG-HF-C and IFG-HF-1). Regardless the digestion procedure, the solutions were transparent and devoid of apparent precipitate following digestion. After

evaporation, the residues were processed through several cycles of dissolution-evaporation with 14N HNO_3 and 12N HCl followed with 7N HNO_3 and 6N HCl until the solutions were stable and clear.

For trace element analyses, the samples were diluted in 40 g of 7N HNO_3. An aliquot of about 2 % of each sample was taken, evaporated to dryness, and re-dissolved in a multi-spiked solution (HNO_3 0.4N + 0.05N HF doped with 10 ppb Be-Ge and 2 ppb In-Tm-Bi) to a dilution factor of 5000. The multi-spiked solution was used to accurately correct the instrumental drift on a large range of masses from ^{3}Be to ^{238}U. Measurements were performed either on an Agilent 7500 Q-ICP-MS or an Agilent 8900 QQQ-ICP-MS at the LMV of Clermont-Ferrand (France). Both instruments are equipped with an inert sample introduction kit, allowing detection of low amounts of High-Field Strength Elements (HFSE) such as Hf. The reference standard BR-24 was measured after every four samples and used to calibrate counts into concentrations through offline data processing. Precision and accuracy were monitored by analyzing the in-house standard BR24 (Polynesian basalt; see Chauvel et al., 2011) that followed the same digestion-dilution protocol as for the samples and was run as an unknown during the sequence. Based on quality control standards (mostly basalt BHVO-2 since no iron-formation standard with sufficiently precise trace-element concentrations is available for quality check), the external reproducibility for trace element concentrations is estimated to be better than 5 % for all trace elements except Cs and Tl that are better than 10 %; Pb better than 15 % and Mo and Cd better than 30 %. Measured BHVO-2 concentrations and instrumental replicate analyses of IF-G and its mineral fractions are in *annexes C.11. et C.12.*

3.2.5. Isotopic compositions

Samarium, Nd, Lu and Hf concentrations were measured by isotope dilution using mixed ^{149}Sm-^{150}Nd and ^{176}Lu-^{178}Hf spikes to calculate precise parent-daughter ratios. Mixed ^{176}Lu-^{178}Hf spikes were specifically prepared and calibrated to determine as precisely as possible high ^{176}Lu/^{177}Hf ratios, between 0.08 to 0.8, usually found in BIF. For Sm-Nd, we used a mixed ^{149}Sm-^{150}Nd spike calibrated for ^{147}Sm/^{144}Nd ratios between 0.05 and 0.8. Based on Sm, Nd, Lu, Hf solutions prepared from ultrapure oxides and metals as well as geological reference materials, we evaluated the precision on ^{176}Lu/^{177}Hf and ^{147}Sm/^{144}Nd ratios at a maximum of 0.5 %. (*c.f. Chapitre 2 section 3.1.3b*) Neodymium, Hf and Pb isotopic compositions were determined from the spiked solutions.

Between 250 and 500 mg of IF-G bulk powder (IFG1 to IFG11) and about 500 mg of the magnetite-rich fraction (Mgt4 to Mgt11) was weighed to obtain enough Hf for isotopic analyses. The silicate-phosphate-carbonate-rich fraction was split into two for dissolution (500 mg for SilD and 300 mg for SilE). Mixed spikes were combined with sample powders and with NH_4HF_2 (ratio 1:4 for sample:flux) right from the beginning of the digestion procedure. Savillex® beakers with sample, mixed spike, and flux were heated in an oven for at least 24 hours at 215°C. The residues were treated through several cycles of dissolution-evaporation in 14N HNO_3 and 12N HCl followed by 7N HNO_3 and 6N HCl until the solutions were stable and clear. Samarium, Nd, Lu, Hf and Pb were isolated and purified using ion chromatography protocol with 7 chromatographic columns (see *Chapitre 2 section 3.2.2.).* Total procedural blanks for Sm, Nd, Lu, Hf and Pb were respectively less than 73, 230, 36, 90 and 290 pg.

All isotopic compositions were measured on a ThermoFisher Neptune Plus MC-ICP-MS at the LMV of Clermont-Ferrand (France). Depending on the amount of element isolated for analyses, either a classical spray-chamber or a desolvator - CETAC Technologies Aridus 3 – were used as an introduction system for measuring Nd and Pb isotopic compositions. The desolvator was systematically used to measure Lu, Hf, and Sm isotopic compositions due to the low amounts of elements available for analyses. For Hf and Nd, instrumental mass bias corrections were performed using the exponential law and ratios of $^{179}Hf/^{177}Hf = 0.7325$ and $^{146}Nd/^{144}Nd = 0.7219$, respectively. The JNdi-1 Clermont-Ferrand Nd and JMC 475 Grenoble Hf reference standards were run every 3 samples during each analytical sequence. The JNdi-1 run using the desolvator at concentrations of 30 and 40 ppb yielded average values of $^{143}Nd/^{144}Nd = 0.512038$ +/- 0.000030 (n = 10, 2SD) and 0.512051 +/- 0.000022 (n = 7, 2SD), respectively. The JNdi-1 run at 200 ppb with the spray chamber yielded an average $^{143}Nd/^{144}Nd$ ratio of 0.512110 +/- 0.000016 (n = 10, 2SD). Altogether, this corresponds to a repeatability of 59 ppm (2SD). Measured $^{143}Nd/^{144}Nd$ ratios were normalized to the recommended value of 0.512099 (Garçon et al., 2018) to correct for residual analytical bias. To match the very low amounts of Hf isolated from the IF-G reference material and its mineral fractions (< 10 ng), we ran the Hf JMC 475 standard at concentrations of 2 and 5 ppb. The 2 ppb JMC 475 standards yielded an average $^{176}Hf/^{177}Hf$ ratio of 0.282141 +/- 0.000077 (n = 3, 2SD), hence a repeatability of about 274 ppm (2SD), while the 5 ppb JMC 475 yielded an average $^{176}Hf/^{177}Hf$ ratio of 0.282158 +/- 0.000028 (n = 12, 2SD), hence a repeatability of about

100 ppm (2SD). All measured $^{176}Hf/^{177}Hf$ ratios were normalized to the recommended value of 0.282160 (Chauvel et al., 2011). (for more details about Lu and Sm measurements, see *Chapitre 2 section 3.3.3. and 3.3.5.*).

For Pb, the instrumental mass fractionation was corrected according to the procedure described by White et al. (2000) using a thallium spike and sample-standard bracketing measuring NBS 981 reference standard after every two samples. The repeatability was determined using repeated measurements of the NBS 981 reference standard. Average values measured for the NBS 981 with the spray chamber (Pb concentration = 150 ppb) and with the desolvator (Pb concentration = 10 ppb) are 16.9542 +/- 0.0022 (150 ppb, n = 38, 2SD) and 16.9358 +/- 0.0010 (10 ppb, n = 5, 2SD) for the $^{206}Pb/^{204}Pb$ ratio; 15.5175 +/- 0.0019 (150 ppb, n = 38, 2SD) and 15.4917 +/- 0.0011 (10 ppb, n = 5, 2SD) for the $^{207}Pb/^{204}Pb$ ratio; 36.7798 +/- 0.0048 (150 ppb, n = 38, 2SD) and 36.6994 +/- 0.0039 (10 ppb, n = 5, 2SD) for the $^{208}Pb/^{204}Pb$. The external repeatability for the NBS 981 reference standard was better than 125 ppm, 152 ppm and 166 ppm for the $^{206}Pb/^{204}Pb$, $^{207}Pb/^{204}Pb$ and $^{208}Pb/^{204}Pb$ ratios, respectively. The residual analytical drift was corrected by normalizing all Pb ratios to the NBS 981 reference values given by Galer and Abouchami (1998).

4. Results

4.1. Petrographic observations

4.1.1. Thin sections

The IF-G reference material, based on the available rock sample, consist of an alternating millimetric to centimetric bands of magnetite (Fe_3O_4), dark bands, and quartz (SiO_2), light-colored bands. In the dark bands, magnetite grains vary in size from 50 to 100 µm and are associated with minor amounts of 100 to 150 µm in size quartz grains (Fig. 2a). In the light-colored bands, quartz grains, 100 to 150 µm in size, dominate, but magnetite is also present as a homogeneously developed < 30 µm in size dusting (Fig. 2b). Under higher magnification, silica-rich bands contain < 30 µm in size magnetite grains as inclusions in quartz as well as 50 to 300 µm in size magnetite clusters at quartz grain boundaries (Fig. 2c). Large actinolite crystals, up to 0.5 to 1 mm in size, are present within the bands, but, more often at the boundary between magnetite-rich and quartz-rich bands, forming mm-thick actinolite-rich bands (Fig. 2a). Numerous 20-40 µm in size

calcite grains are present as inclusion in quartz, mostly in the quartz-rich bands. Apatite grains are developed in the magnetite-rich bands (Fig 2d). The apatite grain shown in Fig.2d is almost 100 µm in size, but the average size of apatite grains is between 10 and 50 µm (*see annexe C.1* for chemical SEM images showing apatite grains).

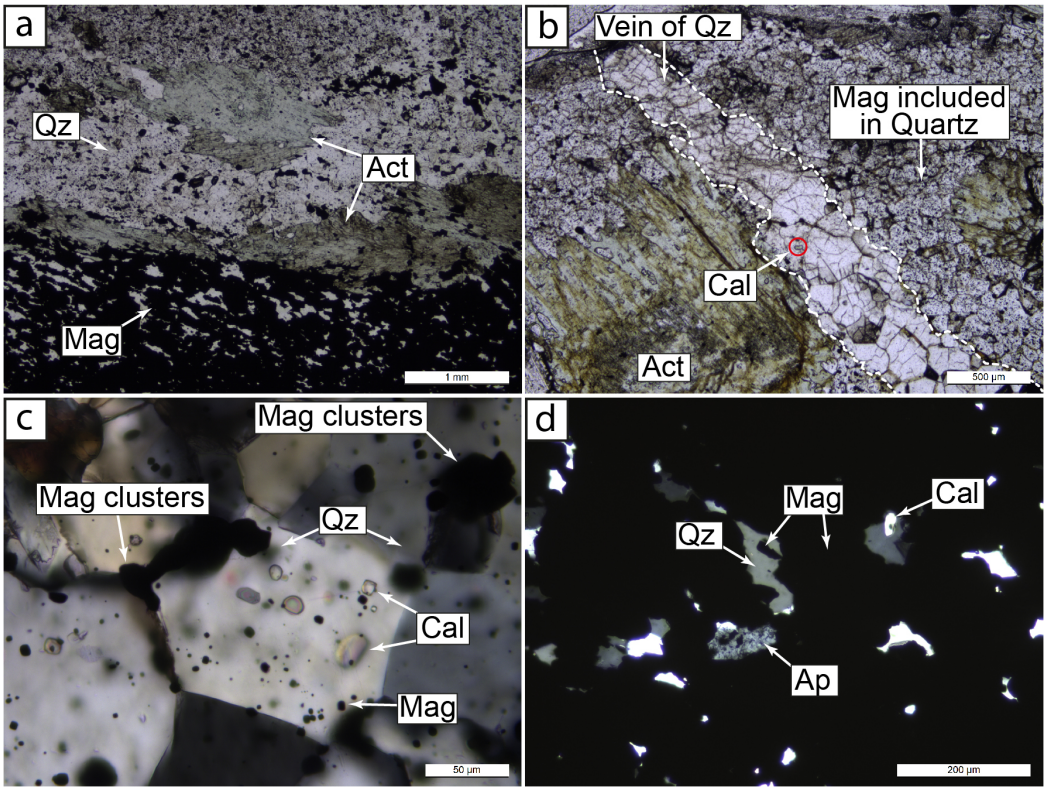

Fig. 2. Photomicrographs of the IF-G sample thin section with (a) Plane-polarized light image of a magnetite-rich and a silica-rich bands separated with an actinolite layer. (b) Plane-polarized light image of a vein filled with 300 µm in size quartz crystals cutting through the silica-rich band. (c) Cross-polarized light close-up image of silica-rich band showing <10 µm in size magnetite crystals and 10 to 40 µm in size calcite inclusions. Magnetite clusters are mainly located at quartz grain boundaries. Quartz crystal joints define 120° angles typical of recrystallized quartz. (d) Cross-polarized light close-up image focused on a 100 µm in size apatite crystal in the magnetite-rich band. Act: actinolite; Qz: quartz; Mag: magnetite; Cal: calcite; Ap: apatite.

A set of 200 µm to 1 mm-wide, quartz-filled veins cuts through both the magnetite-rich and quartz-rich bands at 45° to almost 90° angle (Fig. 2b). Rare, 50 µm in size, euhedral rutile and mm-size euhedral pyrites are developed in the veins. Quartz crystals are larger in the veins than in the quartz-rich bands, having an average size of 300 µm. Few magnetite grains present in the veins appear to be dislodged from the adjacent magnetite-rich bands by fluid circulation and are unlikely to precipitate from the fluid in the veins. The quartz-rich veins also contain calcite and mm-size chlorite crystals, but lack apatite.

4.1.2. Reference material powder

Mineralogy of the IF-G bulk powder is consistent with petrographic observations on thin sections (Fig. 3). Quartz, magnetite, actinolite, calcite, apatite and rare pyrite and cummingtonite (the only mineral not seen in thin sections) are present. Quartz and magnetite are the main components of the BIF (accounting for ~80 %), followed by actinolite (~15 %) and calcite (>3 %). Apatite accounts for 2 % of the mapped surface area and pyrite and cummingtonite for less than 1 %. Actinolite is the third main component of the powder after quartz and magnetite.

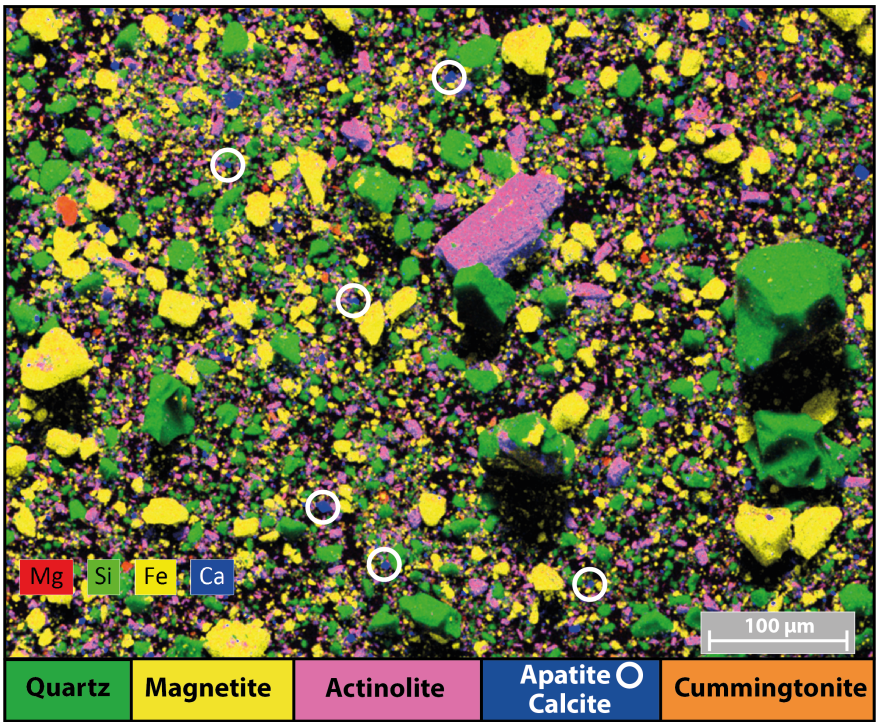

Fig. 3. Chemical SEM image of the IF-G reference material powder. The image shows abundant large grains of actinolite, magnetite and quartz and small grains of calcite, whereas apatite and cummingtonite are rare and small. Chemical acquisition analyses were performed at 15 kV in backscattered electron mode. For simplicity, phosphorus (apatite) and sulfur (pyrite) are not shown on this image, whereas apatite and calcite grains are circled. Phosphorus (P) and Sulfur (S) chemical SEM images are provided in annexe C.2.

According to the certificate of analysis provided by the SARM of Nancy, the IF-G reference material is a powder with a grain-size distribution centered on 80 µm. The observed grain size clearly depends on the mineralogy. If the longest axis length compared, grains show mineral-specific ranges (Fig. 3): actinolite (1-200 µm), quartz (1-100 µm), magnetite (1-50 µm), cummingtonite (1-20 µm), calcite and apatite (1-5 µm) and rare pyrites (<5 µm).

4.2. Major elements

The major element composition of the bulk powder of the IF-G reference material (n = 3) is reported in *annexe C.7*. The BIF standard contains significant amounts of five major elements: SiO_2, Fe_2O_3, MgO, CaO and Al_2O_3. Sodium oxide (Na_2O), K_2O, TiO_2, MnO and P_2O_5 are under 0.05 wt%. The LOI were performed on the two lots and are 1.40 and 1.49 wt%. The average SiO_2 and Fe_2O_{3t} contents are respectively 40.8 ± 1.0 wt% (2SD, n = 3) and 55.4 ± 1.2 wt% (2SD, n = 3) (Fig. 4). The MgO and CaO contents are low, with respective average contents of 1.96 ± 0.06 wt% (2SD, n = 3) and 1.52 ± 0.09 wt% (2SD, n = 3). The Al_2O_3 content is very low with an average of 0.15 ± 0.05 wt% (2SD, n = 3).

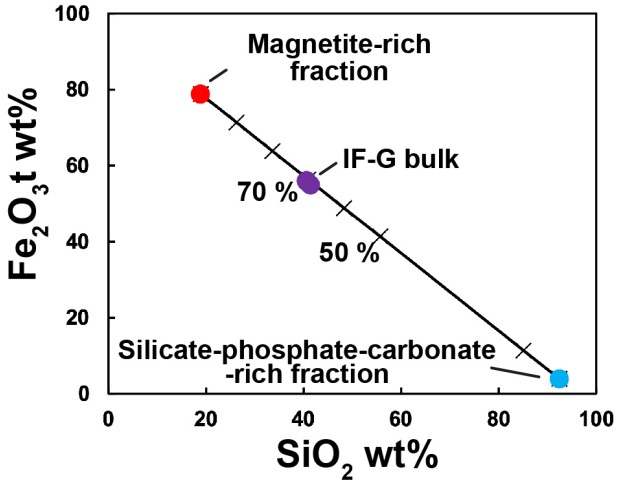

Fig. 4. Fe_2O_{3t} vs SiO_2 content of the IF-G bulk powder (n = 3), the magnetite-rich and the silicate-phosphate-carbonate-rich fractions. The IF-G bulk powder falls along a mixing line indicating that it contains 70 % of magnetite-rich fraction and 30 % of silicate-phosphate-carbonate-rich fraction.

The magnetite-rich fraction separated with a hand-magnet contains 18.9 wt% SiO_2, 78.8 wt% Fe_2O_{3t}, 1.35 wt% MgO and 1.01 wt% CaO. The major element contents of the silicate-phosphate-carbonate-rich fraction with LOI do not add up to 100 wt% – the total is 88.8 wt% with a SiO_2 content of 82.0 wt%. If normalized to 100 %, the silicate-phosphate-carbonate-rich fraction contains 92.4 wt% SiO_2, 3.9 wt% Fe_2O_{3t}, 2.15 wt% MgO and 1.53 wt% CaO. Other major element contents are below detection limits. The SiO_2 vs. Fe_2O_{3t} diagram showing results of mixing calculations indicates that the bulk IF-G powder consists of about 70 % of the magnetite-rich fraction and 30 % of the silicate-phosphate-carbonate-rich fraction (Fig. 4).

4.3. Trace elements

Trace element contents of all analyzed fractions are presented in *annexe C.8 and C.9* as well as BHVO-2 measurements in *annexe C.11*. Trace element contents are shown normalized to the Upper Continental Crust (UCC) of Rudnick and Gao (2014) in Fig. 5a.

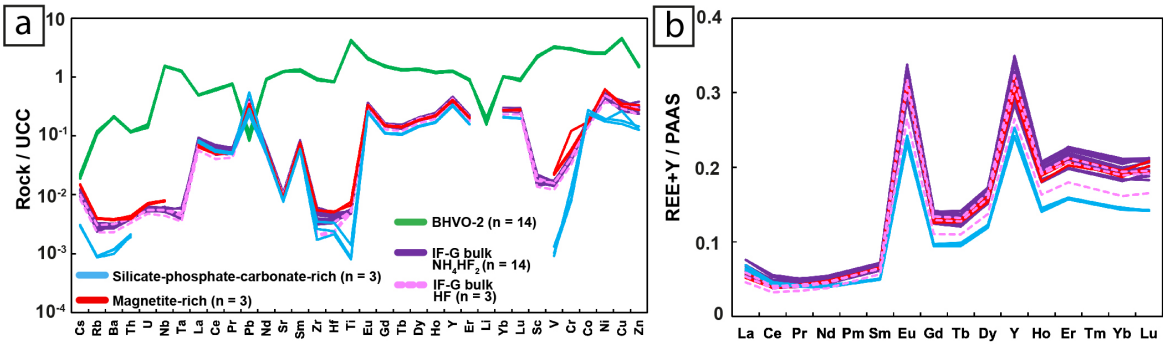

Fig. 5. Trace element composition of the bulk IF-G reference standard and the separated mineral fractions. (a) Multi-element composition normalized to the Upper Continental Crust (UCC) of Rudnick and Gao (2014) *and compared to the BHVO-2 reference standard composition. (b) REE+Y composition normalized to the Post-Archean Australian Shale (PAAS) of* Nance and Taylor (1976).

The IF-G bulk powder has low trace element concentrations, with a general depletion in incompatible elements, relative to the UCC (Fig. 5a). Notably, Sc, V, Cr, Large Ion Lithophile Elements (LILE), such as Cs, Rb, Ba and Th, and High Field Strength Elements (HFSE), with extremely low Zr, Ti and Hf concentrations, are strongly depleted compared to the UCC. Normalized to Post-Archean Australian Shale (PAAS; Nance and Taylor, 1976), the Rare Earth Element (REE) content of the IF-G bulk powder is much lower on average (Σ_{REE+Y} = 20.3 ± 2.7 ppm (2SD, n = 14); Fig. 5b). IF-G is depleted in Light Rare Earth Elements (LREE) with an average $(La/Yb)_{PAAS}$ of 0.31 ± 0.06 (2SD, n = 14). The REE pattern of IF-G shows several positive average anomalies such as a La $(La/La^*)_{PAAS}$ = $(La_{PAAS}/(3Pr_{PAAS} - 2Nd_{PAAS}))$ = 1.67 ± 0.12 (2SD, n = 14), an Eu $(Eu/Eu^*)_{PAAS}$ = $(Eu_{PAAS}/(2/3Sm_{PAAS} + 1/3Tb_{PAAS}))$ = 3.57 ± 0.08 (2SD, n =14), a Gd $(Gd/Gd^*)_{PAAS}$ = $(Gd_{PAAS}/(2Tb_{PAAS} - Dy_{PAAS}))$ = 1.34 ± 0.08 (2SD, n = 14) anomalies and a super-chondritic Y/Ho ratio of 45.4 ± 3.6 (2SD, n = 14). The trace element pattern of the IF-G bulk powder digested with concentrated HF (n = 3) is similar within uncertainties to the IF-G bulk powder digested with NH_4HF_2 (n = 14) except for Zr and Hf concentrations, which are significantly lower (Zr = 0.39 ± 0.03 ppm (2SD, n = 3) and Hf = 14.3 ± 6.7 ppb (2SD, n = 3) in HF-digested powders than in NH_4HF_2-digested powders (Zr = 0.81 ± 0.33 ppm (2SD, n

= 13) and Hf = 21.6 ± 5.0 ppb (2SD, n = 14)). No systematic variability was observed as a function of the amount of powder digested.

The magnetite-rich fractions have trace element patterns very similar to those of the IF-G bulk powders digested with NH_4HF_2, but are slightly enriched in LILE, HFSE and transitional elements (V, Cr, Co and Ni; Fig. 5a). Their HFSE (e.g., Zr, Ti and Hf) contents are 1.05 ± 0.02 ppm (2SD, n = 3), 27.9 ± 4.25 ppm (2SD, n = 3) and 26.7 ± 1.76 ppb (2SD, n = 3), respectively, with significantly higher Ti concentrations than for the bulk powders.

The silicate-phosphate-carbonate-rich fractions are generally depleted in all trace elements compared to the IF-G bulk powders (Fig. 5a). Their HFSE concentrations are very low with the average concentrations of Zr, Ti and Hf of 0.50 ± 0.34 ppm (2SD, n = 3), 3.89 ± 2.53 ppm (2SD, n = 3) and 13.9 ± 6.88 ppb (2SD, n = 3), respectively. These fractions have PAAS-normalized REE patterns very similar, within their uncertainties, to those of the IF-G bulk powders with the average Σ_{REE+Y} concentration of 17.3 ± 0.91 ppm (2SD, n = 3; Fig. 5b). These fractions are slightly more enriched in LREE than the IF-G bulk powders with the average $(La/Yb)_{PAAS}$ ratio of 0.46 ± 0.04 (2SD, n = 3).

4.4. Pb, Lu-Hf and Sm-Nd isotopic compositions

Lead, Hf and Nd isotopic compositions together with Lu, Hf, Sm and Nd concentrations determined by isotope dilution are presented in *Annexe C.13; C.14 and C.15.* The epsilon values were calculated relative to the chondritic uniform reservoir (CHUR) composition given by Bouvier et al. (2008).

4.4.1. Pb-Pb isotopic composition

Nine isotopic analyses of the IF-G bulk powder reveal highly heterogenous and unradiogenic Pb isotopic compositions with $^{206}Pb/^{204}Pb$ ratios varying from 14.7835 to 15.7934, $^{207}Pb/^{204}Pb$ ratios from 14.6874 to 15.0651, and $^{208}Pb/^{204}Pb$ ratios from 34.6893 to 35.6523. Eight analyses of the magnetite-rich fraction vary over a narrower range of Pb isotopic composition, from 14.7152 to 15.1796 for $^{206}Pb/^{204}Pb$, 14.6540 to 14.8329 for $^{207}Pb/^{204}Pb$, and 34.5893 to 35.0559 for $^{208}Pb/^{204}Pb$. The silicate-phosphate-carbonate-rich fraction was analyzed twice for Pb isotope ratios, but the two analyses are

significantly different with $^{206}Pb/^{204}Pb$ ratios of 17.7553 and 15.0076, $^{207}Pb/^{204}Pb$ ratios of 14.6730 and 14.7677 and $^{208}Pb/^{204}Pb$ ratios of 34.6430 and 34.8853.

In the ^{207}Pb-^{206}Pb isotopic space, the bulk-powder analyses (n = 9) define a trend with a slope yielding a ^{207}Pb-^{206}Pb age of 3810 ± 7 Ma, MSWD = 1.06 (Fig. 6a).

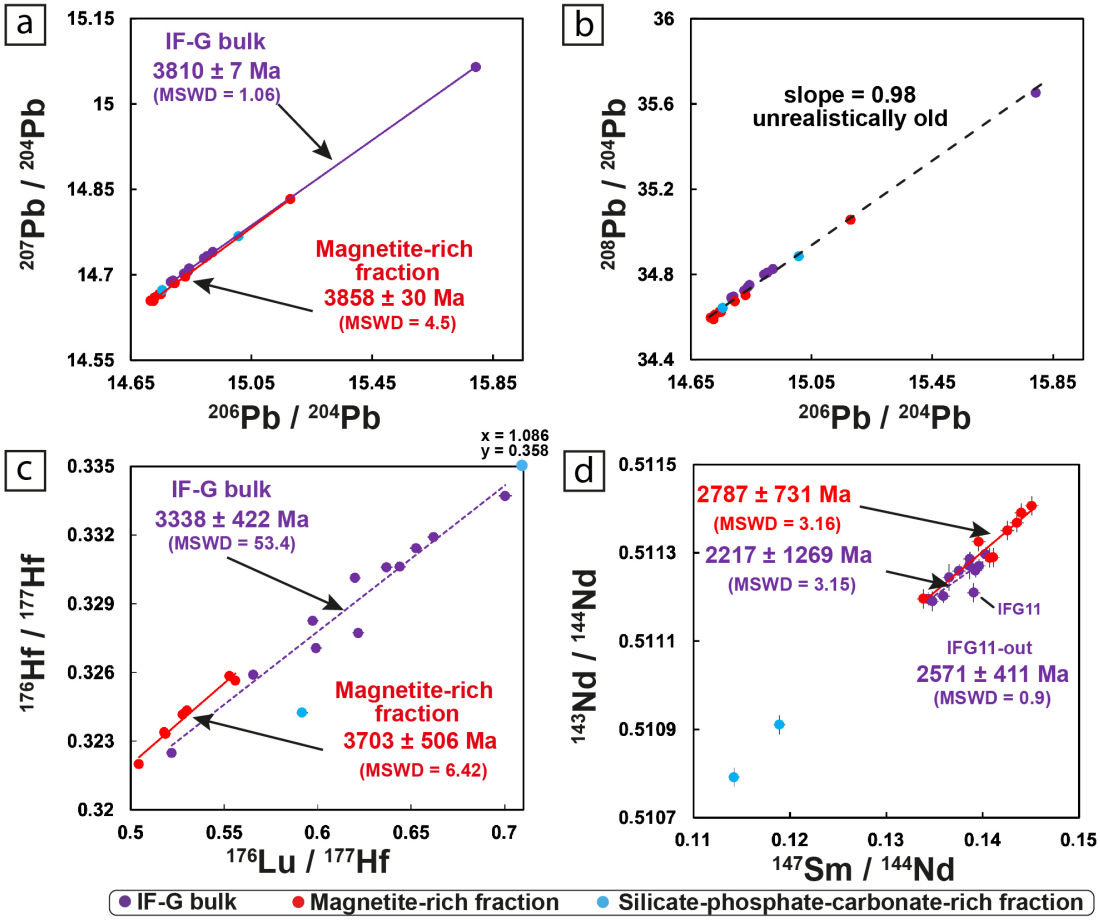

Fig. 6. Radiogenic isotope composition of the bulk IF-G powder, the magnetite-rich and silicate-phosphate-carbonate-rich fractions. (a) $^{207}Pb/^{206}Pb$ isotopic composition. (b) $^{208}Pb/^{206}Pb$ isotopic compositions defining a non-terrestrial age (c) Hf isotopic composition (d) Nd isotopic composition. Error bars are smaller than the point size for most of the datapoints.

Statistical tests show that the slope of the trend is largely determined by the sample with the most radiogenic Pb isotopic composition (i.e., IF-G 10 with $^{207}Pb/^{204}Pb$ = 15.0651 and $^{206}Pb/^{204}Pb$ = 15.7934). Removing this sample from the trend however yields the same age within uncertainties *i.e.,* ^{207}Pb-^{206}Pb age of 3854 ± 65 Ma with a MSWD of 0.95. The magnetite-rich and silicate-phosphate-carbonate-rich fractions fall on the same trend as the bulk IF-G powders in the ^{207}Pb-^{206}Pb isotopic space. The magnetite-rich fraction alone (n = 8) yields an age of 3859 ± 30 Ma with a MSWD of 4.5. Removing sample Mgt11 with

the most radiogenic Pb isotopic composition yields an age of 3828 ± 130 Ma with a MSWD of 5.2. Finally, the two silicate-phosphate-carbonate-rich fractions define a line whose slope gives an age of 3812 ± 25 Ma. Combining the bulk IF-G analyses, the magnetite-rich and silicate-phosphate-carbonate-rich fractions altogether (n = 19) yields an age of 3836 ± 23 Ma (MSWD = 16.5) (Fig. 6a). In the $^{208}Pb/^{204}Pb$ vs. $^{206}Pb/^{204}Pb$ isotopic space, the data define a trend with a slope of 0.98, which is geologically meaningless as it corresponds to a date older than the Earth's formation age (Fig. 6b).

4.4.2. Lu-Hf isotopic composition

Using the isotope dilution technique, average Lu and Hf concentrations of eleven IF-G bulk analyses prepared with NH_4HF_2 are constrained as respectively 92.3 ± 2.0 ppb (2SD) and 21.4 ± 3.9 ppb (2SD), which agree within uncertainties with the average concentrations determined with the ICP-MS multi-spiked solution procedure (see *annexe C.14*). The precision obtained on Lu concentration with the isotope dilution technique is better by a factor of 4 while the precision on Hf concentrations is highly variable within 23 % deviation from the mean value obtained by isotope dilution. The seven spiked magnetite-rich fractions have average Lu and Hf concentrations of 84.6 ± 0.7 ppb (2SD) and 22.9 ± 1.6 ppb (2SD), respectively, which are similar to those for the bulk IF-G powder within uncertainties. The magnetite-rich fraction shows less dispersion for Hf concentration (2SD is 7 %) than the bulk IF-G powder (2SD is 23 %). The two silicate-phosphate-carbonate-rich fractions contain much less Lu (60.7 and 61 ppb) and Hf (8.1 and 14.7 ppb) than the bulk IF-G powder and the magnetite-rich fractions.

The $^{176}Lu/^{177}Hf$ ratios for the eleven IF-G bulk powders are extremely high and variable ranging from 0.5218 to 0.7003. Their present-day $^{176}Hf/^{177}Hf$ isotopic ratios are highly radiogenic and range from 0.322477 to 0.333704 (Fig. 6c). Initial $\varepsilon Hf_{(3.7\ Ga)}$ range from +102.4 to +192.8 for the bulk IF-G powders. The magnetite-rich fractions show generally lower $^{176}Lu/^{177}Hf$ ratios than the bulk IF-G powders with values ranging between 0.5043 and 0.5559 and high $^{176}Hf/^{177}Hf$ isotopic ratios from 0.321990 to 0.325835. Initial $\varepsilon Hf_{(3.7\ Ga)}$ range from +196.1 to +219.7 for magnetite-rich fractions. Propagated analytical errors are estimated between 7.8 and 10.4 $\varepsilon Hf_{(3.7\ Ga)}$ (2SD) for the bulk IF-G powders and magnetite-rich fractions based on the estimated errors on their $^{176}Lu/^{177}Hf$ ratios. One of the two silicate-phosphate-carbonate-rich fractions analyzed (SilD) has shown the highest $^{176}Lu/^{177}Hf$ ratio = 1.0862, a present-day $^{176}Hf/^{177}Hf$ ratio of 0.358152 and a

calculated initial $\varepsilon Hf_{(3.7\ Ga)}$ of 3.0 ± 15.4. The second sample of the silicate-phosphate-carbonate-rich fraction (SilE) yielded an $\varepsilon Hf_{(3.7\ Ga)}$ of 55.2 ± 9.0. The trend defined by the bulk IF-G powders in the field of $^{176}Lu/^{177}Hf$ vs $^{176}Hf/^{177}Hf$ yields an age of 3338 ± 422 Ma with a very high MSWD of 53.4 (Fig. 6c). The trend constrained by the seven magnetite-rich fractions yields an age of 3703 ± 506 Ma with a MSWD of 6.4.

4.4.3. Sm-Nd isotopic composition

The average Sm and Nd concentrations determined by isotope dilution for eleven IF-G bulk powders are respectively 0.391 ± 0.006 ppm (2SD) and 1.716 ± 0.064 ppm (2SD), which agree with the ICP-MS multi-spiked solution analyses (see *annexe C.14*). The magnetite-rich fraction has an average Sm concentration determined by isotope dilution method of 0.351 ± 0.006 ppm (2SD, n = 8) and a larger variability in the Nd concentration of 1.502 ± 0.105 ppm (2SD, n = 8). The two silicate-phosphate-carbonate-rich fractions analyzed show similar lower Sm concentrations of 271.1 and 271.4 ppb and Nd concentrations of 1.378 ppm and 1.436 ppm (see *annexe C.14.)*

$^{147}Sm/^{144}Nd$ ratios for the IF-G bulk powder vary from 0.1343 to 0.1403 (n = 11); those for the magnetite-rich fraction vary from 0.1339 to 0.1451 (n = 8). The two silicate-phosphate-carbonate-rich fractions have lower $^{147}Sm/^{144}Nd$ ratios (0.1142 and 0.1189) than those for the IF-G bulk powder (Fig. 6d). The present-day Nd isotopic composition of the IF-G bulk powder is much less variable than the Hf isotopic composition with an average $^{143}Nd/^{144}Nd$ ratio of 0.511244 ± 0.000077 (2SD, n = 11) and $\varepsilon Nd_{(3.7\ Ga)}$ = + 0.8 ± 1.2 (2SD, n = 11). The magnetite-rich fraction shows higher variability in $^{143}Nd/^{144}Nd$ ratio between 0.511196 and 0.511407 (n = 8), but its $\varepsilon Nd_{(3.7\ Ga)}$ is relatively invariable ($\varepsilon Nd_{(3.7\ Ga)}$ = + 0.7 ± 1.2 (2SD)). The silicate-phosphate-carbonate-rich fraction yielded $^{143}Nd/^{144}Nd$ ratio of 0.510792 and 0.510911 and $\varepsilon Nd_{(3.7\ Ga)}$ = 3.3 (Fig. 6d). The trend defined by the bulk IF-G powders in the field of $^{147}Sm/^{144}Nd$ vs $^{143}Nd/^{144}Nd$ yields an age of 2217 ± 1269 Ma (MSWD = 3.15) and of 2571 ± 411 Ma (MSWD = 0.9) without the sample outlier IFG11 (Fig. 6c). The trend constrained by the seven magnetite-rich fractions yields an age of 2787 ± 731 Ma with a MSWD of 3.16.

5. Discussion

5.1. Standards are never perfect: The "nugget effect" of zircon and apatite might explain geochemical variability of the IF-G reference standard

Preparing a geological reference material (standard) from a rock sample requires a specific protocol to produce a fine powder as representative as possible of the whole sample (Govindaraju, 1984). An average grain-size of a reference material powder after crushing and milling procedures should be under 74 µm according to Jochum et al. (2016). The average grain-size distribution of the IF-G standard is 80 µm according to the certificate of analysis provided by the SARM. Our petrographic observations of the IF-G standard show that the powder still mineralogically inhomogenous with a grain-size dependance on mineralogical composition. SEM imaging (Fig. 3) indicates ubiquitous presence of quartz and magnetite in the BIF standard, but also abundant actinolite, cummingtonite, apatite, calcite and rare pyrite. The actinolite grains show a large range in grain-size up to 200 µm. The smallest grains are apatites ranging from 1 to 5 µm in size.

The IF-G reference material is the only one BIF standard available for purchase. It has been analyzed for trace element concentrations and isotopic compositions in many studies as a quality check for geochemical data (Govindaraju, 1984; Sampaio and Enzweiler, 2015 and references therein). In the certificate of analysis, the SARM recommends to analyse a minimum of 200 mg powder to ensure a good reproducibility for its trace element concentrations. However, none of the fifteen published studies compiled here used such an unusually large amount of powder to perform the analyses (Fig. 7a). Trace element concentrations obtained in this study are within the range of values previously reported for the standard, though literature data are extremely variable for some elements as shown by the calculated deviations in Fig. 7a (*see Annexe C.5 for literature trace element patterns*). For all trace elements, variability exceeds the commonly accepted reproducibility of 5 %, suggesting that the IF-G reference material is not homogenous. Note that particularly low concentrations for most trace elements of the IF-G standard further exacerbate the variability when calculated as relative percentages. Almost all analyses of the IF-G reference material in the literature (n = 17 from 15 publications) are on pre-2006 lots that have been contaminated in crushing facilities for

Cr, Co and W contents (cf. certificate of analysis), consistent with generally higher concentrations for these elements in the literature data (see Fig. 7a; W was not measured in previous studies). Furthermore, V, Nb, Mo and Ta concentrations might be also contaminated as concentrations of these elements seem to be much higher for the pre-2006 lots (see *annexe C.4.* more details).

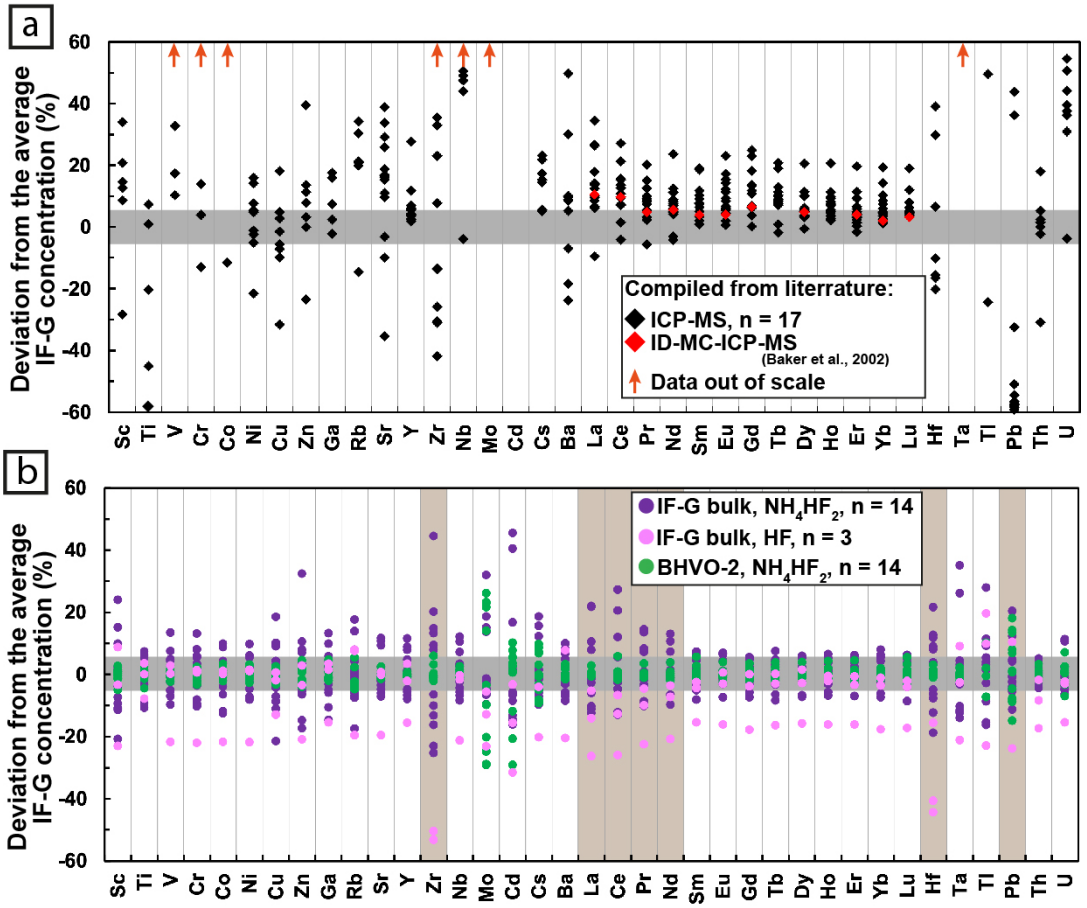

Fig. 7. Variability in trace element concentration of the IF-G reference standard. (a) Deviation in % of the previously published data from the mean reference values defined in the annexe C.10. Orange arrows point that some literature data exceed 60 % deviation. Literature data are from (Govindaraju, 1995; Barrat et al., 2000; Dulski, 2001; Baker et al., 2002; Kamber et al., 2004; Guilmette et al., 2009; Fabre et al., 2011; Parks et al., 2014; Bolhar et al., 2004, 2015; Sampaio and Enzweiler, 2015; Viehmann et al., 2015a, 2015b;Frei et al., 2016; Albut et al., 2018). *(b) Deviation in % of the different bulk IF-G powders analyzed in this study from the mean reference values defined in annexe C.10. The BHVO-2 analyses are also shown for a comparison. For the BHVO-2 standard, deviations are from the mean of all the BHVO-2 analyses from annexe C.11. The brown vertical bands correspond to the element deviations discussed in this study.*

To further investigate sources of variability in our trace element dataset, results for the different methods of dissolution are compared in Fig. 7b. As a reference, we chose to compare IF-G to BHVO-2, a widely used basalt standard recognized for its

reproducibility in terms of trace element content, except for Pb (cf. Chauvel et al., 2011). Precision for all BHVO-2 trace element analyses generally falls in a range of ± 5 % around the mean value except for Mo, Cd, Cs, Tl and Pb, due to their low abundances in BHVO-2 and/or instrumental limitations. In contrast, precision for IF-G analyses is rarely below 5 %, rather close to 10 % on average. Even less reproducible concentrations, showing deviations from the mean value above 20 %, are measured for Sc, Zn, As, Zr, Mo, Cd, La, Ce, Hf, Ta, Tl, Pb, and U. Light REE such as La and Ce show generally more variability than HREE (Fig. 7b). The high variability in concentrations of elements known to be difficult to measure with ICP-MS could be partly – or mostly – accounted for by analytical limitations (i.e., Sc, Zn, Mo, Cd and Tl). The poor reproducibility of Hf, LREE, and Pb concentrations is of direct concern to our study since their isotopic compositions were analyzed. In our dataset, deviations of Zr and Hf concentrations from the IF-G reference values which is defined in *annexe C.10.* are strongly correlated (Fig. 8a) as are the deviations of La and Ce (Fig. 8b). Deviations of La and Zr are however not correlated, indicating that LREE, Zr and Hf are not hosted by the same mineral phases (Fig. 8c). Lead concentrations are not correlated with either Zr or La concentrations (c.f. *annexe C.3.*). This indicates that Pb is not hosted by the same minerals that host Zr and LREE. Given mineralogical heterogeneity and coarse grain-size of the powder, poor reproducibility of our IF-G trace element data might reflect a "nugget effect". A nugget effect is observed when some mineral grains have higher trace element content than other mineral grains (Kurfürst et al., 1993).

Regarding La and Ce, large variability between duplicate analyses of the IF-G bulk powder might be due to apatite presence. Small apatite grains, 1 to 5 µm in size, are present at the level of a few % in both the IF-G thin sections and powder. Lepland et al. (2002) observed that apatite has 100 times higher LREE content than actinolite in BIFs of the Snowpatch Formation. Lack of correlation between the deviations of Ti and LREE concentrations from the IF-G reference values (Fig. 8d) indicates that rutile does not control LREE content. Quartz, pyrite, cummingtonite and calcite carry low content of LREE and cannot explain large La and Ce variabilities (Garçon et al., 2014; Large et al., 2014; Lepland et al., 2002; Allwood et al., 2010; Kamber et al., 2014). The REE patterns and concentrations of apatite strongly depends on its origin: magmatic, diagenetic or hydrothermal (Lepland et al., 2002; Nishizawa et al., 2005; Nutman & Friend, 2006; Puchelt & Emmermann, 1976). Lepland et al. (2002) identified an apatite population from the

Snowpatch Formation BIFs with flat chondrite-normalized REE+Y patterns that are sufficiently enriched in La and Ce to induce a nugget effect for these two elements. Since Sm and Nd have electronic configurations similar to those of La and Ce, and Nd is well correlated to La (*see annexe C.3.*), apatite might also play a major role in the Sm and Nd budgets of the IF-G reference material. On the other hand, absence of clear correlation between Pb and either La or Zr suggests that the Pb budget of the IF-G reference material is not controlled by apatite or zircon.

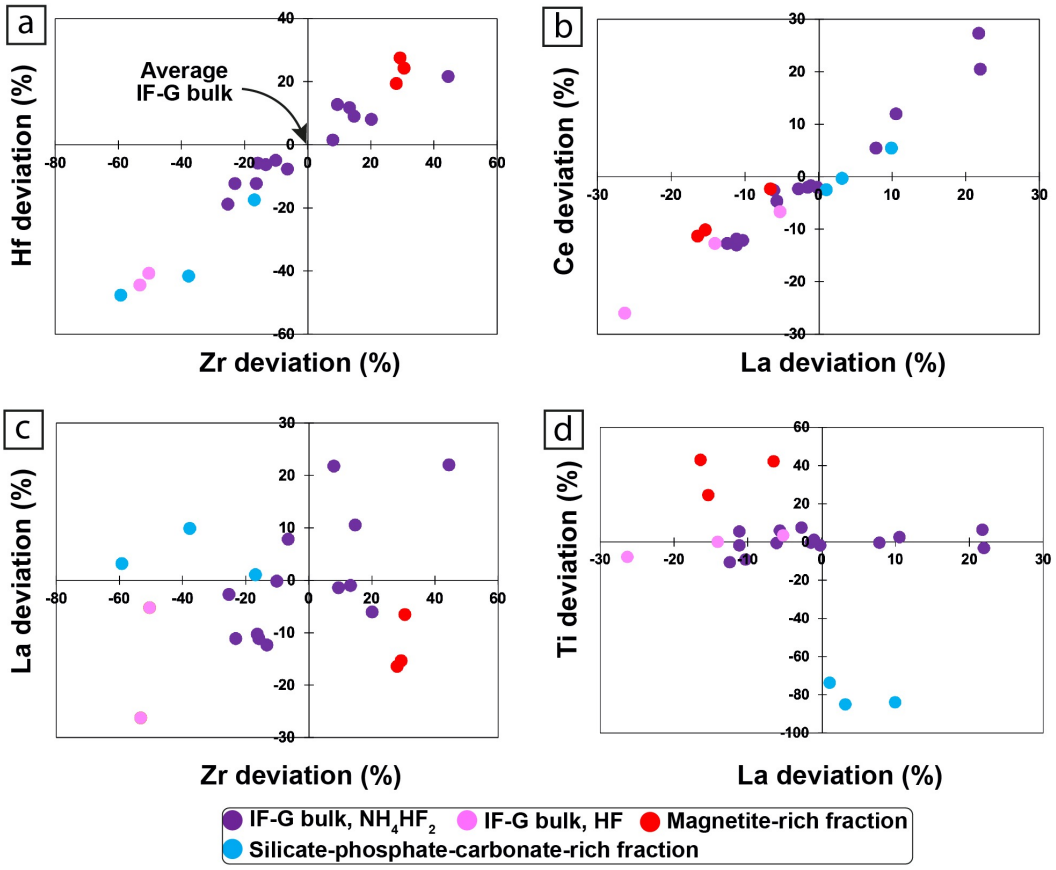

Fig.8. Deviation of each IF-G measurement and mineral fractions from the average composition of the IF-G reference material as defined in annexe C.10. (a) Deviation of Hf vs Zr. (b) Deviation of Ce vs La. (c) Deviation of La vs Zr. (d) Deviation of Ti vs La.

The Zr and Hf concentrations measured for the HF-digested powders (Fig. 7b) are systematically lower than those for the NH_4HF_2-digested powders. Incomplete digestion of small zircons present in the IF-G powder might explain this pattern since the digestion protocol using NH_4HF_2 at >200°C efficiently digests zircon-rich rocks (Zhang et al., 2012). To test this hypothesis and to imitate the incomplete digestion of zircons, about 800 mg of IF-G bulk powder was digested with 2N HF at 90 °C temperature for a day. The mixture

was then centrifuged, the residue was digested with NH_4HF_2 and analyzed for trace element concentrations with ICP-MS (see the detailed procedure in *annexe C.6.*). The residue has trace element characteristics similar to those of zircons with a REE pattern strongly enriched in HREE compared to LREE with $(La/Yb)_{PAAS}$ ratio of 0.0045 vs. 0.31 ± 0.06 (2SD, n = 14) for the bulk IF-G powders, a lower Th/U ratio of 1.57 vs. 2.78 ± 0.31 (2SD, n = 14) for the bulk powders and a much higher Zr concentration and Zr/Th ratio of 1210 for the residue vs. 19.2 ± 7.8 (2SD, n = 14) for the IF-G bulk powder. The $^{176}Lu/^{177}Hf$ ratio of the residue (0.035) is also significantly lower, and closer to that of zircon, than that for the bulk IF-G powders (0.56 ± 0.11, 2SD, n = 14). The bulk Zr/Hf ratio of the IF-G powder digested with NH_4HF_2 (37.5 ± 6.9, 2SD, n = 13) also supports presence of zircons in the IF-G standard. This value is similar, within error, to that for the average upper continental crust (Zr/Hf = 36; Rudnick and Gao, 2014) in which zircon is the main host of Zr and Hf. By contrast, modern seawater (Zr/Hf = 56-207; Bau, 1996; Godfrey et al., 1996, 2008; Firdaus et al., 2008), marine hydrogenetic ferromanganese crust (Zr/Hf = 50-90, Bau, 1996; Bau and Koschinsky, 2009; Schmidt et al., 2014), and detritus-free BIF (e.g., FeR-3 BIF reference material with Zr/Hf = 54; Bau and Alexander, 2009) have much higher Zr/Hf ratios because Zr and Hf are not hosted in zircons in these reservoirs.

Several independent geochemical lines of evidence therefore strongly suggest presence of zircons in the IF-G standard. Petrographic observations in thin sections and in the powder by Raman spectroscopy and SEM imaging failed to identify them and therefore these “phantom” zircons are likely to be small, on the order of tens to hundreds of nanometers, or too dispersed. However, several studies reported that rare zircons were separated from metacherts and BIFs of the BIF Member of the Snowpatch Formation (Nutman et al., 2007, 2009). Presence of zircons is somewhat unexpected for BIFs having as low Zr and Hf concentrations as the IF-G reference material (Zr = 0.81 ppm and Hf = 21.6 ppb). The structural formula of zircon indicates that it contains 50 wt% of zirconium (Zr). Assuming that Zr is entirely hosted in zircon in the IF-G standard, mass balance indicates that the proportion of ‘phantom zircon’ cannot exceed 0.00016 wt%, explaining why it was not observed petrographically. Using this maximum proportion and a Zr/Hf ratio of 37.5 for the IF-G bulk powder, zircon also accounts for 100 % of the Hf budget in the bulk powder (estimated Hf concentration of about 22 ppb vs. 21.6 ppb measured). Using REE concentrations measured in a zircon fraction by Garçon et al. (2014), such a low proportion of zircons would only contribute to 0.1 % of HREE budget (based on Yb)

and less than 0.002 % of the LREE budget (based on La) of the IF-G bulk powder, hence should have no impact on the REE patterns and REE budget of the BIF.

In light of these results, the IF-G standard is not ideal to be used as a reference material for trace element concentrations due to its mineralogical and geochemical heterogeneities. *Annexe C.10* presents the average trace element concentrations for the IF-G bulk powder with associated precisions based on the 12 duplicate analyses where at least 100 mg were digested with NH_4HF_2.

5.2. Multiple radiogenic ages for the IF-G reference material: What do they mean?

5.2.1. Depositional age of the BIF

Previous studies reported rare zircons in BIFs of the Snowpatch Formation, including the sampling locality of the IF-G reference material. The few zircons about 50 µm in size yielded an U-Pb crystallization age of ca. 3695 Ma (Nutman et al., 2009). The ca. 3695 Ma zircons have stubby prismatic oscillatory-zoning, high Th/U ratios and negative Eu anomalies indicating their co-precipitation with plagioclase. Nutman et al. (2009) interpreted the zircons as being the products of volcanogenic activity, potentially ashfalls. They interpreted the depositional age of the BIFs to be contemporaneous with volcanic activity at ca. 3695 Ma.

Previously published whole-rock Pb isotopic composition of the Snowpatch Formation BIFs from the same area and their leached fractions also yielded the Eoarchean ^{207}Pb-^{206}Pb isochron dates at ca. 3.7 Ga, though some of them were initially interpreted as metamorphic rather than depositional ages. The Snowpatch Formation BIFs were first dated at 3760 ± 70 Ma (MSWD = 1) by Moorbath et al. (1973), based on a ^{207}Pb-^{206}Pb isochron on bulk samples. Later, Frei et al. (1999) dated hand-picked magnetite from the Snowpatch Formation BIFs at 3691 ± 22 Ma (MSWD = 0.4), based on a ^{207}Pb-^{206}Pb isochron. A third ^{207}Pb-^{206}Pb isochron dating of mesobands of the Snowpatch Formation BIFs yielded a date of 3691 ± 49 Ma (Frei & Polat, 2007). Based on the published literature (whole-rock ^{207}Pb-^{206}Pb isochron dates and U-Pb dates for zircon), the Snowpatch Formation BIFs, including the IF-G reference material, were deposited during the Eoarchean ca. 3.7 Ga ago, in agreement with the proposed age for the inner arc of the Isua Greenstone Belt (Nutman and Friend, 2009; Nutman et al., 2022).

5.2.2. Age of the detrital 'phantom zircons'

The Pb isotopic composition of the IF-G standard measured in this study, in particular their ^{207}Pb-^{206}Pb date (Fig. 6a), confirms that this isotopic systematics traces processes of the Eoarchean age. The slope of the linear trend defined by our 9 duplicate analyses of the bulk IF-G powder however provides an age about 100 Ma older (3810 ± 7 Ma, MSWD = 1.06; Fig. 6a) than the ^{207}Pb-^{206}Pb isochron dates obtained in previous studies as discussed in the above section. The slope of the trend defined by the 8 duplicate analyses of the magnetite-rich fraction separated from the IF-G reference powder is even slightly older giving a date of 3858 ± 30 Ma (MSWD = 4.5).

The 'phantom zircons' of the IF-G reference material (c.f. Section 5.1) might have acted as a time capsule to preserve the primary Pb isotopic signature of the Snowpatch Formation BIFs. Zircon is a very resistant and highly U-enriched mineral that develops extremely radiogenic ^{207}Pb/^{204}Pb and ^{206}Pb/^{204}Pb ratios through time. Zircons do not host high amounts of Pb, which explains why Zr and Pb concentrations do not co-vary in duplicate analyses of IF-G (see *annexe C.3.*), but their extremely radiogenic Pb isotopic composition, ^{207}Pb/^{204}Pb and ^{206}Pb/^{204}Pb ratios up to 4 orders of magnitude higher than those for common lead, has a strong influence on the bulk isotopic composition of the IF-G reference material. As in previous studies, our ^{208}Pb-^{206}Pb isochron dates defined by the bulk IF-G powder and mineral fractions have no geological meaning since they are older than the formation age of the Earth (Fig. 6b). This isotopic feature is consistent with a major control of zircons on ^{207}Pb-^{206}Pb isotopic composition because zircon does not contain as much Th as U, hence has far less influence on the radiogenic product of ^{232}Th that is ^{208}Pb.

To test this interpretation, theoretical Pb isotopic composition of a 3.81 Ga zircon was calculated. Since initial Pb and U contents of zircons at the time when they crystallized is not known, a range of possible U and ^{204}Pb concentrations (e.g. Garçon et al., 2014; Nutman et al., 1997b) was tested to account for some of the most extreme cases seen in the literature. As a result, $^{206\text{-}207}$Pb isotopic composition of zircons having ^{204}Pb concentration of 2 or 20 ppb and initial U content of 30 or 500 ppm was estimated (Fig. 9a). A mixing between these zircons and the least radiogenic $^{207\text{-}206}$Pb isotopic composition measured for the IF-G standard in this study has then been modelled (Fig. 9a). The important result of this exercise is that, whatever the amount of U and ^{204}Pb was initially present in the zircons, the mixing line defines a linear trend determined by both

the bulk IF-G powder and the magnetite-rich fraction. This indicates that the presence of only 0.00001 to 0.01 wt% zircons in the bulk IF-G powder and the magnetite-rich fraction can explain the whole range of measured Pb isotopic composition. Such low proportion of zircons is in line with that estimated from the trace element concentrations (see previous section 5.1, in which a maximum proportion of 0.00016 wt% zircon was estimated). The ^{207}Pb-^{206}Pb date of 3810 ± 7 Ma with a MSWD of 1.06 is therefore interpreted as the average age of the zircons in the IF-G reference material.

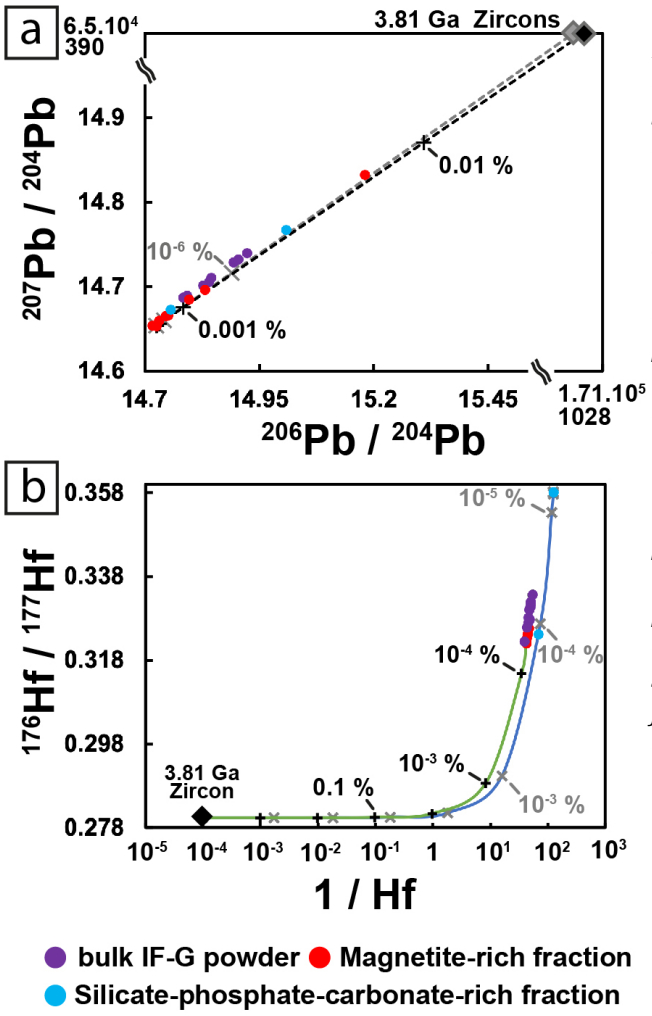

Fig. 9. Variability of Pb and Hf isotopic composition modelled as mixing with ca. 3.81 Ga zircons. (a) Pb-Pb isotopic composition. Dashed lines represent mixing lines between the least radiogenic magnetite-rich fraction (Mgt 8) and a 'phantom zircon' formed 3.81 Ga ago. The light-grey mixing line was calculated for a zircon containing 500 ppm of U and 2 ppb of ^{204}Pb. The black mixing line was calculated for a zircon containing 30 ppm U and 20 ppb ^{204}Pb. (b) Hf isotopic composition. The green mixing line was calculated between a 'phantom 3.81 Ga zircon' containing 80 ppm of Lu and 1 wt% Hf and the most radiogenic composition of the bulk IF-G powder (IFG7). The blue mixing line was calculated with the most radiogenic silicate-phosphate-carbonate-rich fraction (SilD). Ticks indicate contribution of 'phantom zircons' to the mixture following a power of 10.

The age must correspond to the average age of the detrital zircons in the BIF of the Snowpatch Formation from which the IF-G standard originated. The zircons could be either of volcanogenic origin or derived from an emerged landmass that had 3.81 Ga and older rocks exposed (consistent with 3814 ± 12 Ma and 3850 ± 12 Ma detrital zircon ages from the underlying Conglomerate Member; Nutman et al., 2009). There are no known

3.81 Ga rocks in the Northeastern Isua Inner Arc, but the zircons could have been derived from the outer arc, assuming that the studied BIF was deposited in a basin developed between the two arcs, or from the entirely recycled Inner Arc rocks. Thus, our study suggests detrital contribution to BIFs of the Snowpatch Formation, pointing to an emerged landmass with ca. 3.81 Ga and older rocks that are not known in the study area.

5.2.3. Lu-Hf and Sm-Nd isochron ages

A surprising feature of this isotopic dataset is that the bulk IF-G standard powder and the mineral fractions yielded younger Lu-Hf and Sm-Nd isochron ages, with high MSWD, than the ^{207}Pb-^{206}Pb isotopic system (Fig. 6c-d). Lead is more mobile in fluids and during metamorphism than Sm, Nd, Lu and Hf (Rudnick and Gao, 2014) so it is uncommon for Archean rocks to preserve primary signals in their Pb isotopic signatures.

Bulk IF-G powder and the magnetite-rich fraction provide Lu-Hf isochron dates of 3338 ± 422 Ma (MSWD = 53.4; n = 11) and 3703 ± 506 Ma (MSWD = 6.42; n = 7), respectively (Fig. 6c). These dates are consistent with the assumed depositional age of the studied BIFs, but the age uncertainty and the dispersion of the datapoints around the linear trend are high (MSWD >> 1). Such a high MSWD may indicate that the Lu-Hf isotopic system has been disturbed by post-depositional metamorphic events and/or that the mineral phases controlling the Hf isotopic composition are not cogenetic, for example resulting from mixing of minerals derived from different sources. To test the later interpretation, geochemical modeling has been performed to evaluate zircon contribution to the Hf isotopic composition of the IF-G reference material. Zircons are highly enriched in Hf so this mineral should exert a strong control on Hf isotopic composition of the IF-G reference material. However, Lu-bearing mineral phases such as apatites might also significantly contribute to the Hf isotopic budget of the IF-G reference material and its Lu/Hf ratio. To model the contribution of zircon, theoretical Hf isotopic composition of a 3.81 Ga zircon with Hf concentration of 10000 ppm and a $^{176}Lu/^{177}Hf$ of 0.001 was calculated (Garçon et al., 2014) (Fig. 9b). Then a mixing between this theoretical zircon and material with the most radiogenic Hf isotopic composition measured in the duplicate analyses of the IF-G bulk powder and mineral fractions was modelled. The proportion of zircon required to explain the whole range of measured Hf isotopic composition is in the same range as the one needed to explain the ^{207}Pb-^{206}Pb isotopic system i.e. around 0.0001 and 0.00001 wt%. This correspondence suggests that variable zircon amount in

the duplicate analyses of the IF-G bulk powder could account for the wide range of their Hf isotopic composition, hence the poor reproducibility of the standard despite large sample aliquots (between 250 and 500 mg for each duplicate). The full range of Hf isotopic composition measured in magnetite-rich and silicate-phosphate-carbonate-rich fractions can be explained in the same way. Notably, based on petrological observations and trace element analyses, these mineral fractions are far from being pure magnetite or silicate-phosphate-carbonate endmembers. The conclusion is thus that none of the Hf isotopic compositions measured in this study represent a pure seawater-precipitate endmember. They rather reflect different degree of mixing between zircons and other mineral phases (e.g., iron oxides, apatites) that could be either primary or secondary. Therefore, the large age uncertainties and high MSWD values associated with the Lu-Hf isochron dates of the bulk IF-G standard powder and magnetite-rich fraction (Fig. 6c) are interpreted to be a direct consequence of mixing of non-cogenetic mineral phases contributing in various proportions to the Hf isotopic composition.

Bulk IF-G powder and magnetite-rich fraction yielded Sm-Nd isochron dates of 2571 ± 411 Ma (MSWD = 0.9, n = 10, without outlier IF-G 11) and 2787 +/- 731 Ma (MSWD = 3.16, n = 8), respectively (Fig. 6d). These dates are much younger that the assumed depositional age of the studied BIFs (i.e., 3.7 Ga), although with large uncertainties. Large variability in LREE concentrations between the duplicate analyses of the IF-G reference material suggests that apatite played a major role in defining their Nd isotopic composition. Lepland et al. (2002) and Nishizawa et al. (2005) reported two generations of apatite from the Snowpatch Formation BIFs based on in-situ REE analyses. First generation of apatite has relatively flat REE patterns that were interpreted to reflect chemical sedimentary origin and seawater composition. The second apatite generation has MREE-enriched or LREE-depleted patterns interpreted to reflect precipitation from carbonate-rich metasomatic fluids. Based on Sm and Nd apatite concentrations published by Nishizawa et al. (2005) and trace element patterns published by Lepland et al. (2002),the first apatite generation has $^{147}Sm/^{144}Nd$ ratios between 0.11 and 0.13, while the second apatite generation has higher $^{147}Sm/^{144}Nd$ ratios at around 0.2-0.3. Our analyses of the IF-G reference material yielded $^{147}Sm/^{144}Nd$ ratios between 0.134 and 0.140, significantly higher than those of the silicate-phosphate-carbonate-rich fraction (0.114 and 0.119) and lower than those of the magnetite-rich fraction with one sample excluded (>0.14; Fig. 6c). The Nd isotopic composition of the IF-G standard thus seems to

reflect a mixture of two source components that could be the two apatite generations identified by Lepland et al. (2002). Note that the resetting of the Sm-Nd isotopic system of the Snowpatch Formation BIF has been inferred in previous studies (Frei et al., 1999; Frei and Polat, 2007; Miller and O'Nions, 1985; Shimizu et al., 1990). In conclusion, the Sm-Nd isochron dates (Fig. 6d) likely reflect both mixing and post-depositional, metamorphic events and hence have no geological meaning as indicated by their large uncertainties.

5.3. Is there a geochemical meaning for the extremely radiogenic initial Hf isotopic composition of the Isua BIF and its magnetite-rich fraction?

Interpreting an initial Hf isotopic composition of the Isua BIF, or any other rock, in term of sources requires that the isotopic system remained closed to any addition and loss of parent and daughter elements since the deposition of the sediments. One way to check if this is indeed the case is to verify that the Lu-Hf isochron dates defined by a suite of cogenetic rocks or minerals yield geologically meaningful ages. In the previous section, it has been suggested that the trends seen in Fig. 6c are due to mixing of magnetite with zircon and potentially two generations of apatite with different Lu and Hf concentrations that are unlikely to be cogenetic. Therefore, there is no way to evaluate whether the initial Hf isotopic compositions are meaningful from a geological point of view.

Initial Hf isotopic composition calculated at 3.7 Ga for the bulk IF-G powder yields extremely radiogenic values up to $\varepsilon Hf_{(3.7\ Ga)}$ of +102.4 to +192.8 with propagated errors estimated to be < 10 $\varepsilon Hf_{(3.7\ Ga)}$ (*see annexe C.14.*). The $^{176}Lu/^{177}Hf$ ratios of the bulk IF-G powder are >0.5, much higher than those for any other silicate rock on Earth, indicating substantial contribution of radiogenic Hf to the present-day $^{176}Hf/^{177}Hf$ ratio of the IF-G standard and making initial **ε**Hf values critically dependent on the radiogenic correction. The present-day Hf isotopic composition of IF-G is $\varepsilon Hf_{(0)}$ = +1637 ± 225 (2SD, n = 11). Considering its $^{176}Lu/^{177}Hf$ ratio of 0.620 ± 0.097 (2SD, n = 11), **ε**Hf value increases by 40 units every 100 Ma. The main sources of error in the calculated initial isotopic composition are the parent-daughter ratio, $^{176}Lu/^{177}Hf$ ratios, and the depositional age. The mixed Lu-Hf spikes used in this study were specifically calibrated for BIFs and thus guarantee the best possible precision on the $^{176}Lu/^{177}Hf$ ratio. Propagation of the error on

the $^{176}Lu/^{177}Hf$ ratios (i.e., 0.5%) cannot explain the extremely radiogenic values measured for the IF-G standard as it amounts to a maximum of 10 $\varepsilon Hf_{(3.7\ Ga)}$ units. The age at which the Hf isotopic composition is calculated is more critical. Calculating initial Hf isotopic composition at 3.81 Ga (the ^{207}Pb-^{206}Pb isochron date obtained in this study) yields less radiogenic initial **ε**Hf, on average +109 $\varepsilon Hf_{(3.81\ Ga)}$, but they are still unrealistic. The magnetite-rich fraction has initial $\varepsilon Hf_{(3.7\ Ga)}$ even higher than that for the bulk IF-G powder as they range between +196.1 and +219.7.

Very radiogenic initial **ε**Hf values have commonly been reported for the Archean BIFs from several localities (Viehmann, 2018), including 2 Isua BIF samples presumably from the ca. 3.75 Ga Dividing Sedimentary Unit (Fig. 1) for which $\varepsilon Hf_{(3.7\ Ga)} > +30$ were calculated (Blichert-Toft et al., 1999). Viehmann (2018) interpreted this highly radiogenic Hf isotopic signature, decoupled from initial Nd isotopic compositions, as primary Archean seawater composition alike that for modern seawater. This composition could reflect the zircon-free Hf isotopic composition of felsic continents, in other words contribution of radiogenic Hf released from minerals other than zircon during weathering of emerged continents. This peculiar isotopic signature is then taken as an evidence for the presence of large felsic, emerged continental landmasses in the Archean (Viehmann, 2018).

To the best of our knowledge, the $\varepsilon Hf_{(3.7\ Ga)}$ of the IF-G reference material constrained in this study are the highest ever reported for an Archean BIF so far. Explaining these values by the contribution of radiogenic mineral phases to the Hf isotopic budget of seawater calls for extreme scenario implying the presence of large emerged continental landmasses in the Hadean, which is not supported by existing constraints (e.g. Flament et al., 2013). Given the potential influence of secondary apatites on Lu concentration and Lu/Hf ratio of the IF-G reference material and its magnetite-rich fraction, it seems more likely that metamorphic events disturbed the Lu-Hf isotopic system.

5.4. A word of caution about the use and meaning of 'typical seawater trace element signature'

The shape and anomalies of the REE+Y patterns normalized to post-Archean Australian shales (PAAS; Nance and Taylor, 1976) are often used to evaluate whether BIF deposits record the geochemical signature of ancient seawater and can be used as an archive to study Archean surface conditions (Bolhar et al., 2004). The IF-G standard displays the archetype signature of a genuine Archean seawater precipitate devoid of terrigenous input (Bau et al., 1996; Bolhar et al., 2004; Friend et al., 2008). Amongst these typical geochemical features are a depletion of LREE relative to the HREE, a general REE+Y-depletion compared to shales (PAAS) associated with low HFSE and Al contents, indicating the lack or low content of detrital aluminosilicates, and the well-defined positive La, Gd, Eu and Y anomalies (Figs. 5a, b). Positive Eu anomalies are attributed to larger contribution of Eu-rich, reduced high-temperature hydrothermal fluids to the global seawater budget (Bau & Dulski, 1999; Bau & Moller, 1992; Michard, 1989). Positive La, Gd and Y anomalies are due to a particular electronic configuration and complexation behavior of these elements that enhance their stability in solution (seawater) compared to other REEs (De Baar et al., 1991, 1985; Bau et al., 1996; Bolhar et al., 2004).

The Sm-Nd and Lu-Hf isotopic composition of the studied bulk IF-G reference powder and the separated mineral fraction are disturbed by metamorphic events (see Sections 5.2.3. and 5.3.) and cannot be reliably interpreted as a seawater signature. Furthermore, the presence of 'phantom zircons' in the bulk IF-G reference powder challenges the interpretation that low HFSE content in BIFs (even on the order of a 1 ppm) is a criterion to rule out contribution of terrigenous input. While the proportion of zircons in the IF-G reference material is extremely low, probably on the order of 0.0001 - 0.00001 wt%, they impose a significant control over the Pb and Hf isotopic compositions of the BIF. The effect of 'phantom zircon' on HFSE concentrations and Hf-Pb isotopic composition of BIFs should therefore be considered in future BIF studies.

6. Conclusions

The study provides petrographic and geochemical (trace element and Pb, Hf and Nd isotope) analyses of the IF-G reference material, which is one of the oldest BIF deposits known on Earth so far. The IF-G reference material was sampled from the BIF Member of the Snowpatch Formation in the Northeastern Isua Greenstone Belt (Greenland), which has been affected by an amphibolite grade metamorphism. The IF-G reference material however serves as a reference for trace element concentrations and is thought to record typical features of ancient seawater, in particular its REE-Y patterns.

The key conclusions of this study can be summarized as follows:

- The IF-G reference material is highly heterogenous in terms of grain size, mineralogy, and geochemistry. Our results suggest that the nugget effect of apatite and zircon explain the poor reproductivity of its trace-element concentrations and Pb, Nd and Hf isotopic composition.

- The duplicated analyses of the bulk IF-G powder provide a well-defined ^{207}Pb-^{206}Pb isochron date of 3810 ± 7 Ma (MSWD = 1.06), which is about 110 Ma older than the presumed depositional age of the BIF. Based on binary mixing calculations, this date might correspond to the average age of the zircon population hosted in the BIF. The age difference highlights a potential detrital contribution from >3.8 Ga emerged landmass that has not yet been documented in the Inner Arc of the Isua Greenstone Belt.

- The initial Hf isotopic composition of the IF-G reference material and its magnetite-rich fraction yield unrealistically high radiogenic values at 3.7 Ga, with $\varepsilon Hf_{(3.7\ Ga)}$ between +100 and +250. Highly radiogenic **ε**Hf values are often reported for the Archean BIFs and interpreted to reflect weathering of large emerged landmasses of felsic continental crust. Instead, these values might reflect variable contribution of volcanic and detrital zircons and primary and secondary apatites, affecting the Lu/Hf ratio of BIFs.

- Finally, the results of this study challenge the notion that the typical seawater-like REE-Y patterns associated with low Zr and Al concentrations in chemical sediments such as BIFs guarantee minimal contribution of terrigenous material to this geochemical archive and excellent preservation of primary seawater signatures, including that of radiogenic isotope composition.

Acknowledgement

We thank C. Cloquet (SARM Nancy, France) for sending us a hand sample of the reference material for petrographic study and C. Constantin (LMV, Université Clermont Auvergne) who prepared thin sections. C. Bosq (LMV, Université Clermont Auvergne) helped to ensure optimal conditions in the clean lab of the LMV. We thank C. Fonquernie (LMV, Université Clermont Auvergne) who carried major element analyses; J.L. Piro, M. Neimard and A.M. Gannoun (LMV, Université Clermont Auvergne) for their technical contribution during ICP-MS and MC-ICPMS measurements; E. Voyer and E. Gardés (LMV, Université Clermont Auvergne) for their technical contribution to maintain the LMV SEM instrument and assistance in powder analyses to search zircons; F. Schiavi for her help and guidance to identify mineral phases with RAMAN spectrometry. This study was funded by the European Research Council (ERC Starting Grant – GOforISOBIF, Grant agreement N°852239). This is a contribution no. to the ClerVolc program of the International Research Center for Disaster Sciences and Sustainable Development at the University of Clermont Auvergne. A.B. acknowledges support from the Petroleum Foundation of the American Chemical Society grant 624840ND2.